Selection of special orientations in relativistic collisions of deformed heavy nuclei

C. Nepali, G. Fai, and D. Keane
Center for Nuclear Research, Department of Physics
Kent State University, Kent, OH 44242, USA
(Dated: February 1, 2008)

We have studied U+U collisions at $\sqrt{s_{NN}} = 200$ GeV using Monte Carlo Glauber, UrQMD and AMPT models. We find that it is possible to separate central tip-tip events as well as central body-body events on the basis of cuts on multiplicity and magnitude of the reduced flow vector.

PACS numbers: 25.75.-q, 24.10.Lx

I. INTRODUCTION

One of the recent surprises about the properties of the QCD matter formed in Au+Au collisions at RHIC is that it appears to flow with near-zero viscosity: an almost perfect liquid [1, 2, 3, 4, 5, 6]. This is in contrast with prior expectations of non-interacting gas-like behavior, and is based in part on approximate agreement between results from non-viscous hydrodynamic calculations and experimental data on elliptic flow. Azimuthal anisotropy in the transverse plane, or elliptic flow (v_2), is sensitive to the early pressure developed in the system and its equation of state. There is a close connection between elliptic flow and the initial spatial eccentricity (ϵ) of the transverse overlap region of the two colliding nuclei. Non-viscous hydrodynamic calculations predict constant v_2/ϵ over a wide range of impact parameters [1]. While the data remain well below the non-viscous hydrodynamic values at lower beam energies, central collisions of Au+Au at $\sqrt{s_{NN}} = 200$ GeV just reach the prediction [4, 7].

In relativistic uranium-uranium (U+U) collisions, there is the potential to produce more extreme conditions of excited matter (higher density and/or a greater volume of highly excited matter) than is possible using spherical nuclei like Au+Au or Pb+Pb at the same incident energy [8, 9, 10, 11, 12]. However, this potential can be partly lost if we have limited capability to distinguish experimentally between different collision orientations when the ions interact near zero impact parameter. The prior studies cited above have devoted attention to this problem, and while there is agreement that U+U collisions offer worthwhile advantages over Au+Au, quantitative particulars have yet to be worked out in detail [10, 11, 12]. Furthermore, U+U collisions offer the opportunity to explore a different and wider range of initial eccentricities than is possible in the case of Au+Au. Among the possible collision orientations, of particular interest are the "tip-tip" orientation, in which the long axes of both deformed nuclei are aligned with the beam axis, and the "body-body" orientation, in which the long axes are both perpendicular to the beam axis and parallel to each other. In this paper, we report a study of the selection of these orientations based on a Monte-Carlo Glauber model [13, 14], Ultra-relativistic Quantum Molecular Dynamics (UrQMD 1.3) [15], and A Multi Phase Transport Model (AMPT v1.11-v2.11) [16].

The Glauber model is solely based on collision geometry [13]. The UrQMD model is a microscopic transport theory based on the covariant propagation of all hadrons on classical trajectories in combination with stochastic binary scatterings, color string formation and resonance decay [15]. We use this model with default settings. AMPT is a hybrid model. It uses the heavy-ion jet interaction generator (HIJING) to generate initial conditions, Zhang's parton cascade (ZPC) for the partonic scattering and hadronization, and a relativistic transport (ART) model for hadronic interactions and freeze-out [16]. We use this model with string melting, where all excited strings that are not projectile and target nucleons without any interactions are converted to partons according to the flavor and spin structures of their valence quarks. This option with appropriate partonic cross-section gives higher value of elliptic flow, close to the experimental value, than without string melting [16]. We keep all other options at their default settings.

The article is organized as follows: in Sec. II, we briefly review the relevant quantities and outline our calculation, and in Sec. III, we present the selection procedure for tip-tip and body-body events and discuss the results. In Sec. IV, we summarize our findings.

II. CALCULATIONAL FRAMEWORK

We represent the quadrupole deformation of the ground-state uranium nucleus in the standard [17] way: we take a Saxon-Woods density distribution with surface thickness $a = 0.535$ fm and with $R = R_{\rm sp}(0.91 + 0.27\cos^2\theta)$, where θ is the polar angle relative to the long axis of the nucleus and $R_{sp} = 1.12\ A^{1/3} - 0.86\ A^{-1/3}$ fm [17]. The small hexadecapole moment of the uranium nucleus is neglected. This yields $R_{\rm long}/R_{\rm perp} \approx 1.29$ [12]. The orientation of the first and second nucleus in the colliding pair is fixed by the two angles (θ_p, ϕ_p) and (θ_t, ϕ_t), respectively. The angles θ_p and θ_t describe the orientation of the long axis relative to the beam direction, and they are uniformly distributed in $[0,\ \pi/2]$. The azimuthal angles ϕ_p and ϕ_t describe rotations about the beam direction, and they are uniformly distributed in $[0,\ 2\pi]$. The Monte-Carlo Glauber simulation is as described in Ref. [12], and charged multiplicity in the

central pseudo-rapidity region is parametrized using the approach of Ref. [18]:

$$\frac{dN_{\rm ch}}{d\eta}\Big|_{\eta=0} = n_{\rm pp}\,[x\,N_{\rm b} + (1-x)\,\frac{N_{\rm w}}{2}]\,, \qquad (1)$$

where $n_{\rm pp} = 2.19$ and $x = 0.15$ are obtained by fitting the PHOBOS data [19] for Au+Au at 200 GeV [12]. Here, $N_{\rm b}$ and $N_{\rm w}$ are the number of binary collisions, and number of participant (wounded) nucleons, respectively. The multiplicity is then distributed according to a negative binomial [20] in order to get a realistic distribution. To convert between track densities in rapidity y, and pseudo-rapidity η, we use the approximation $dN_{\rm ch}/dy \approx 1.15\ dN_{\rm ch}/d\eta$ [21] in the Monte-Carlo Glauber calculations. The UrQMD and AMPT codes have been modified to simulate the deformed uranium nuclei.

In this paper, "ideal tip-tip" and "ideal body-body" refer to the configurations in which the long axes of both deformed nuclei are aligned with the beam axis at zero impact parameter ($\theta_p = \theta_t = \phi_p = \phi_t = 0,\ b = 0$ fm) and in which the long axes are both perpendicular to the beam axis and parallel to each other at zero impact parameter ($\theta_p = \theta_t = \pi/2,\ \phi_p = \phi_t = 0,\ b = 0$ fm), respectively [9, 12]. As the statistical weight of the above mentioned ideal configurations is negligible, "tip-tip" and "body-body" are used to refer to the configurations close to "ideal tip-tip" and "ideal body-body", respectively, for selection purposes.

In the standard way of calculating the spatial eccentricity of the transverse overlap region, $\epsilon_{\rm std}$, the minor axis of the ellipse representing the transverse overlap region is taken along the direction of the impact parameter. However, the minor axis may not be along the direction of the impact parameter due to fluctuation in the participating nucleon positions [22]. The spatial eccentricity calculated by taking into account the rotation of the minor axis is referred to as the participant eccentricity, $\epsilon_{\rm part}$, and given by Ref. [22]:

$$\epsilon_{\rm part} = \frac{\sqrt{(\sigma_y^2 - \sigma_x^2)^2 + 4\sigma_{xy}^2}}{\sigma_y^2 + \sigma_x^2}\,, \qquad (2)$$

with

$$\sigma_x^2 = \langle x^2\rangle - \langle x\rangle^2\,, \qquad \sigma_y^2 = \langle y^2\rangle - \langle y\rangle^2\,, \qquad (3)$$

$$\sigma_{xy} = \langle xy\rangle - \langle x\rangle\langle y\rangle\,, \qquad (4)$$

where x and y are the transverse coordinates of the participant nucleons and angle brackets denote averaging over participant nucleons in a single event. For spherical nuclei, the difference between $\epsilon_{\rm std}$ and $\epsilon_{\rm part}$ is significant only in smaller systems or smaller overlap regions [22]. However, in case of collisions of deformed nuclei, the transverse overlap region may not be an ellipse depending on the collision configurations. Because of this, the difference between $\epsilon_{\rm std}$ and $\epsilon_{\rm part}$ is significant even in central collisions. We use $\epsilon_{\rm part}$ in our calculations.

The area of the transverse overlap region is given by

$$S = \pi\sqrt{\sigma_x^2\,\sigma_y^2}\,. \qquad (5)$$

The event flow vector for the second harmonic, $\vec{Q}_2$, is defined as [23]

$$\vec{Q}_2 = \sum_k^{n_{ch}} \hat{i}\,w_k\,\cos 2\phi_k\ + \sum_k^{n_{ch}} \hat{j}\,w_k\,\sin 2\phi_k\ . \qquad (6)$$

We also use the corresponding reduced flow vector, whose magnitude is

$$q_2 = |\vec{Q}_2|/\sqrt{n_{ch}\langle w_k^2\rangle} = |\vec{Q}_2|/\sqrt{\sum_k^{n_{ch}} w_k^2}\ , \qquad (7)$$

where ϕ_k is the azimuthal angle of a particle, w_k is a weighting factor for that particle, and the summation is over all $n_{\rm ch}$ charged particles in the event. The magnitude of the reduced flow vector, q_2 as defined above, is used in this work to establish a measure of flow strength where the trivial dependence on $n_{\rm ch}$ is removed [21]. The transverse-momentum-integrated elliptic flow, v_2, is parameterized as $v_2 = 0.034\,\epsilon_{\rm part}\,(dN_{\rm ch}/dy)^{1/3}$ [24], where $dN_{\rm ch}/dy$ is the central rapidity density of the charged particles. This expression is known to give a good description of Au+Au collisions at $\sqrt{s_{NN}} = 200$ GeV and we assume here that it also holds for U+U collisions.

To include v_2 in the Glauber model, azimuthal angles ϕ for $2(dN_{\rm ch}/d\eta)$ tracks are generated according to the above parametrization, and we take $w_k = 1$. In the UrQMD and AMPT models, $w_k = p_k^{\perp}$ for $p_k^{\perp} \le 2.0$ GeV/c and $w_k = 2.0$ GeV/c otherwise, where $p_k^{\perp}$ is the transverse momentum of the $k^{\rm th}$ particle in the event.

The quantities S and $\epsilon_{\rm part}$ for all the above-mentioned models were calculated on the basis of the Glauber model. The transverse particle densities, $(1/S)(dN_{\rm ch}/dy)$ [11, 12] for ideal cases are:

$$\frac{1}{S}\frac{dN_{\rm ch}}{dy}\Big|_{y=0} \approx \begin{cases} 43.9\,{\rm fm}^{-2} & \text{ideal tip-tip}\,, \\ 31.0\,{\rm fm}^{-2} & \text{ideal body-body}\,. \end{cases} \qquad (8)$$

III. SELECTION PROCEDURE

The calculations based on the models show that the U+U central tip-tip configuration has the smallest overlap area, similar to central Au+Au, and results in the highest multiplicity. It is a good candidate to create the highest possible $(1/S)(dN_{\rm ch}/dy)$ at any given beam energy. The higher the multiplicity, the better the applicability of hydrodynamics calculations [25]. The central body-body configuration also yields higher multiplicity than average, but smaller $(1/S)(dN_{\rm ch}/dy)$, similar to central Au+Au, due to its large overlap area. However, it produces larger elliptic flow at the same $(1/S)(dN_{\rm ch}/dy)$.

The tip-tip configuration yields higher $(1/S)(dN_{\rm ch}/dy)$ at similar ϵ, and the body-body configuration yields higher ϵ at similar $(1/S)(dN_{\rm ch}/dy)$, compared to Au+Au at the same beam energy. For comparison of the selected events with the ideal cases, we fitted the S and $(1/S)(dN_{ch}/dy)$ distributions for ideal tip-tip and ideal body-body configurations with Gaussians. The quantity q_2 for ideal tip-tip is fitted according to [21]:

$$\frac{dP}{q_2\, dq_2} \propto \frac{1}{\sigma_2^2}\, \exp\left(-\frac{v^2 2M + q_2^2}{2\sigma_2^2}\right) I_0\left(\frac{q_2 v_2 \sqrt{M}}{\sigma_2^2}\right)\,, \quad (9)$$

with

$$\sigma_2^2 = 0.5\,(1+g_2)\,, \quad (10)$$

where I_0 is the modified Bessel function, $M = dN_{ch}/d\eta$, and v_2 is the elliptic flow. The quantities v_2 and g_2 are taken as free parameters in fitting. The participant eccentricity, $\epsilon_{\rm part}$, is fitted similarly with different values of g_2. For ideal body-body, a Gaussian fits well.

The following characteristics of the tip-tip and body-body configurations are used for selection:

$$\text{tip-tip} \Longrightarrow \begin{cases} \text{largest } dN_{ch}/d\eta \text{ (central collisions)}\,, \\ \text{smallest } q_2\,, \text{ i.e., smallest } \epsilon_{\rm part}, \text{ and} \\ \text{smallest } S\,; \end{cases} \quad (11)$$

and

$$\text{body-body} \Longrightarrow \begin{cases} \text{largest } dN_{ch}/d\eta \text{ (central collisions)}\,, \\ \text{largest } q_2\,, \text{ i.e., largest } \epsilon_{\rm part}, \text{ and} \\ \text{largest } S\,. \end{cases} \quad (12)$$

The selected events are compared to the ideal cases. While S and $\epsilon_{\rm part}$ cannot be directly measured, they are compared to the ideal cases for identification purposes.

A. Tip-tip

The quantity $N_{\rm w}$ is approximately the same in tip-tip and body-body configurations because both have full overlap. However, $N_{\rm b}$ is larger in tip-tip than body-body. Because of the contribution from $N_{\rm b}$, the multiplicity is larger in tip-tip than body-body collisions. Thus, it is possible to select tip-tip on the basis of multiplicity only. However, for a variety of reason, this approach has relatively poor efficiency, and instead we have used both multiplicity and the reduced flow vector.

To select tip-tip events, first we take the top 1% $dN_{\rm ch}/d\eta$ to select full overlap configurations. These are already rich in tip-tip, but a further selection of the bottom 25% q_2 is taken from the above subset to further enhance the tip-tip configuration. Figs. 1, 2, and 3 show the event distributions for the above three models, after cuts, compared with the ideal tip-tip case. The transverse particle density, $(1/S)(dN_{\rm ch}/dy)$, obtained after these cuts is ≈ 40 fm^{-2}, which is significantly larger than Au+Au at the same beam energy.

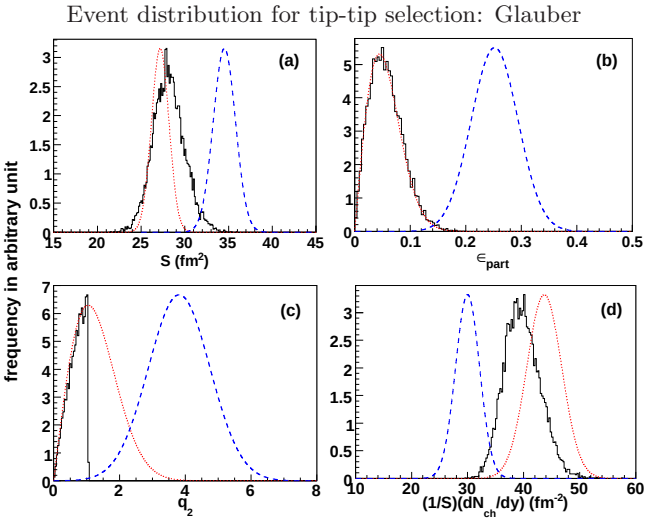

FIG. 1: (Color online) Distribution of (a) transverse overlap area, (b) eccentricity of the transverse overlap region, (c) magnitude of the reduced flow vector, and (d) transverse particle density from Monte-Carlo Glauber. The y-axes have arbitrary units. The dotted and dashed curves are fitted for ideal tip-tip and ideal body-body configurations respectively, compared here with the selected tip-tip events (solid lines).

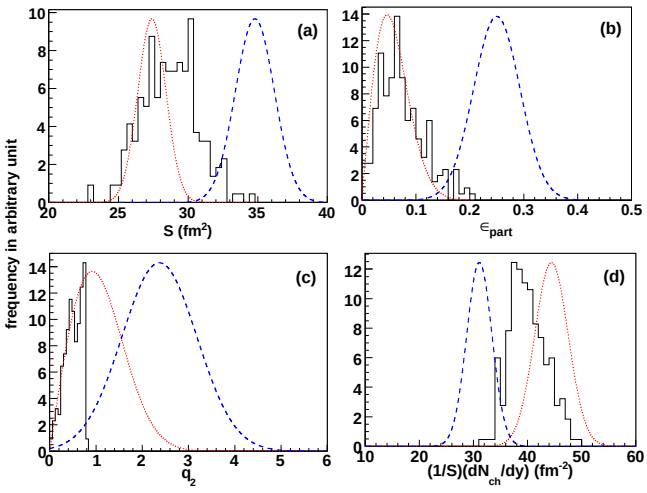

FIG. 2: (Color online) Same as Fig. 1 for UrQMD.

B. Body-body

Here, we first take the top 3% $dN_{\rm ch}/d\eta$ to select full overlap configurations. Then we take the top 1% q_2 to select body-body events. The $(1/S)(dN_{\rm ch}/dy)$ obtained after all these cuts is ≈ 33 fm^{-2}. Figs. 4, 5, and 6 show the event distributions, after cuts, compared with the ideal body-body case, for the three models.

We have also tested an alternative procedure: take the top 3% $dN_{ch}/d\eta$ to select full overlap events. Then, take

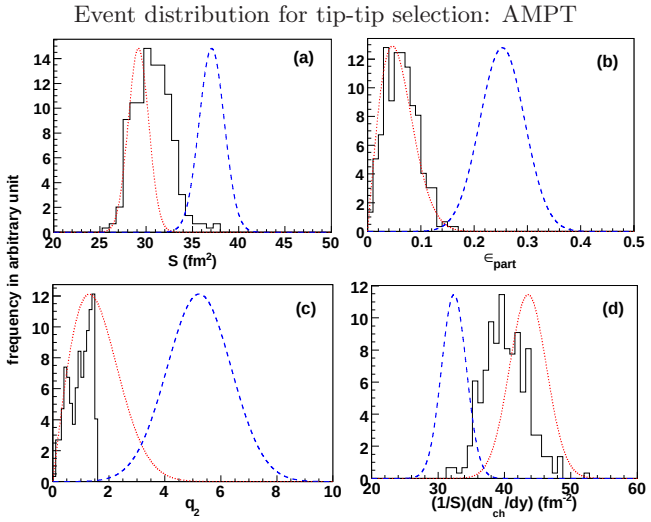

FIG. 3: (Color online) Same as Fig. 1 for AMPT.

the lower 50% $dN_{ch}/d\eta$ from the above subset to select mostly body-body events. This sample is further purified by taking the top 5% q_2. However, this method is less efficient than the one discussed above.

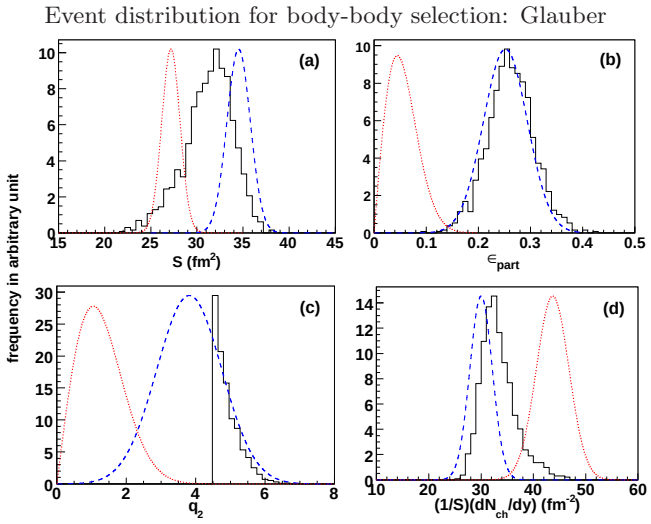

FIG. 4: (Color online) Same as Fig. 1 for selected body-body events in the Glauber model.

C. Discussion

The center of the S distribution in the ideal tip-tip and the ideal body-body from AMPT (Fig. 3(a) and Fig. 6(a)) differs from that for the Glauber model (Fig. 1(a) and Fig. 4(a)) and for UrQMD (Fig. 2(a) and Fig. 5(a)) because of a different parametrization of the nuclear radius used in AMPT compared with the

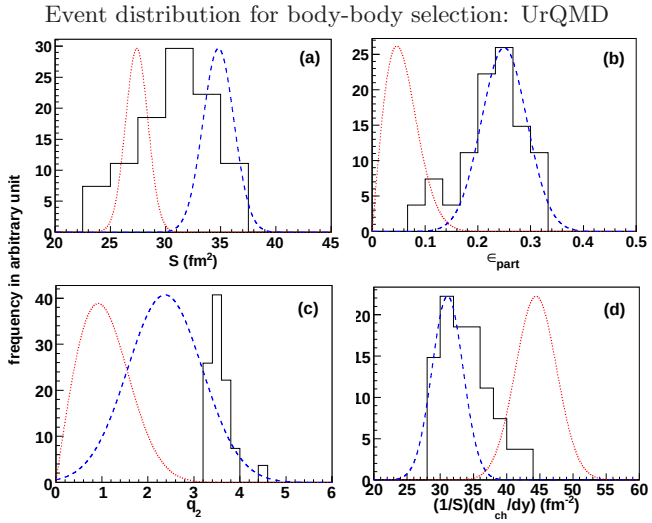

FIG. 5: (Color online) Same as Fig. 1 for selected body-body events in the UrQMD model.

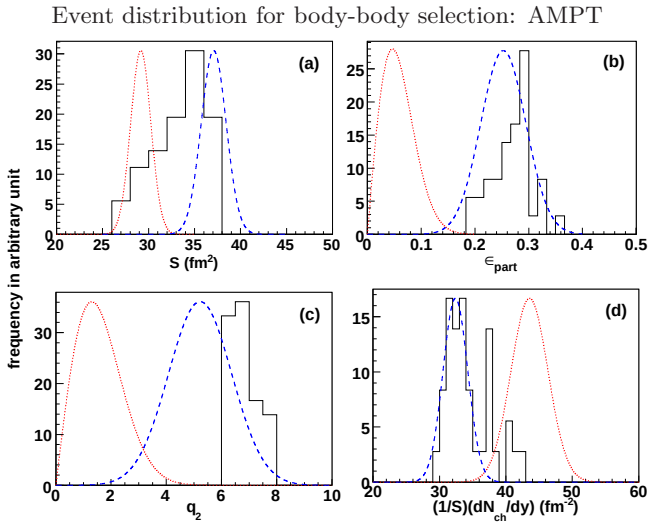

FIG. 6: (Color online) Same as Fig. 1 for selected body-body events in the AMPT model.

other two models. The $\epsilon_{\rm part}$ distributions for the selected events from all models are in good agreement with the ideal cases for both tip-tip (Fig. 1(b), Fig. 2(b), Fig. 3(b)) and body-body (Fig. 4(b), Fig. 5(b), Fig. 6(b)) selections. The quantity q_2 is sensitive to $\epsilon_{\rm part}$ and because of this, the hard cuts on q_2 bring the selected sample closer to the ideal values.

The $dN_{ch}/d\eta$ cut selects mostly tip-tip events, with some body-body as well as other event categories having smaller $\epsilon_{\rm part}$ but larger S, depending on the orientation of the nuclei. The additional cut in q_2 helps to remove most of the body-body events, but still leaves some events with smaller $\epsilon_{\rm part}$ but larger S. That is why the S distribution for the selected events is a little different from the

ideal cases. The selection purity can be further improved by applying an even harder cut in $dN_{ch}/d\eta$. A similar argument is also applicable to the body-body selection.

IV. SUMMARY AND CONCLUSION

U+U collisions at maximum RHIC energy are predicted by three rather different models to produce more extreme excitation of nuclear matter than has been achieved to date using Au+Au. The expected benefits of colliding U+U include a closer approach to the conditions where hydrodynamics should be applicable, and the opportunity to explore a different and wider range of initial eccentricities than is possible in the case of Au+Au. However, we can achieve the full potential benefits of U+U collisions only if we are able to select favored collision orientations.

The parameter space explored by colliding deformed nuclei is more varied than for spherical nuclei. The tip-tip U+U configuration offers higher $(1/S)(dN_{\rm ch}/dy)$, and lower v_2 (similar to central Au+Au). The body-body configuration gives higher v_2, and lower $(1/S)(dN_{\rm ch}/dy)$ (similar to central Au+Au).

We have presented a prescription for selection of tip-tip and body-body configurations, based on the experimental observables $dN_{ch}/d\eta$ and q_2. The $\epsilon_{\rm part}$ values for the selected events are in very good agreement with the ideal cases in all models, although S is somewhat different. In our previous study [12], we have estimated the benefits of U+U collisions including the effect of detector resolution. Here we have used a wider set of kinematic variables to demonstrate that the desired configurations can be selected efficiently. With the development of the Electron Beam Ion Source (EBIS) [26], we expect U+U collisions at RHIC in the not-too-distant future.

V. ACKNOWLEDGMENT

We thank Paul Sorensen for helpful ideas and discussions. We also thank Peter Jacobs for useful discussions. This work was supported in part by U.S. DOE grants DE-FG02-86ER40251 and DE-FG02-89ER40531.

[1] P. F. Kolb and U. W. Heinz, In Hwa, R.C. (ed.) *et al.*: *Quark-Gluon Plasma 3*, p. 634-714, arXiv:nucl-th/0305084.
[2] U. W. Heinz, In Ellis, N. (ed.) *et al.*: *2002 European School of high-energy physics, Pylos, Greece, 25 Aug-7 Sep 2002 Proceedings*, p. 127-178; arXiv:hep-ph/0407360.
[3] P. F. Kolb, U. W. Heinz, P. Huovinen, K. J. Eskola and K. Tuominen, Nucl. Phys. A **696**, 197 (2001).
[4] J. Adams *et al.* [STAR Collaboration], Nucl. Phys. A **757**, 102 (2005).
[5] T. Hirano and M. Gyulassy, Nucl. Phys. A **769**, 71 (2006).
[6] M. J. Tannenbaum, Rept. Prog. Phys. **69**, 2005 (2006).
[7] S. A. Voloshin [STAR Collaboration], *19th International Conference on Ultra-Relativistic Nucleus-Nucleus Collisions: Quark Matter 2006 (QM2006), Shanghai, China, 14-20 Nov 2006*; arXiv:nucl-ex/0701038.
[8] E. V. Shuryak, Phys. Rev. C **61**, 034905 (2000).
[9] B. A. Li, Phys. Rev. C **61**, 021903 (2000).
[10] U. W. Heinz and A. Kuhlman, Phys. Rev. Lett. **94**, 132301 (2005).
[11] A. J. Kuhlman and U. W. Heinz, Phys. Rev. C **72**, 037901 (2005).
[12] C. Nepali, G. Fai and D. Keane, Phys. Rev. C **73**, 034911 (2006).
[13] R. J. Glauber *Lectures on Theoretical Physics*, Interscience, New York, 1959, Vol. I.
[14] J. Adams *et al.* [STAR Collaboration], arXiv:nucl-ex/0311017.
[15] S. A. Bass *et al.*, Prog. Part. Nucl. Phys. **41**, 225 (1998); M. Bleicher *et al.*, J. Phys. G **25**, 1859 (1999).
[16] Z. W. Lin, C. M. Ko, B. A. Li, B. Zhang and S. Pal, Phys. Rev. C **72**, 064901 (2005); Z. W. Lin, S. Pal, C. M. Ko, B. A. Li and B. Zhang, Phys. Rev. C **64**, 011902 (2001); B. Zhang, C. M. Ko, B. A. Li and Z. w. Lin, Phys. Rev. C **61**, 067901 (2000).
[17] A. Bohr and B. R. Mottelson, *Nuclear Structure*, Vol. I, page 161 and Vol. II, page 133 (Benjamin, New York, 1969).
[18] D. Kharzeev and M. Nardi, Phys. Lett. B **507**, 121 (2001).
[19] B. B. Back *et al.* [PHOBOS Collaboration], Phys. Rev. C **65**, 061901 (2002).
[20] R. E. Ansorge *et al.* [UA5 Collaboration], Z. Phys. C **43**, 357 (1989).
[21] C. Adler *et al.* [STAR Collaboration], Phys. Rev. C **66**, 034904 (2002).
[22] S. Manly *et al.* [PHOBOS Collaboration], Nucl. Phys. A **774**, 523 (2006); S.A. Voloshin, *Proc. of 22nd Winter Workshop on Nuclear Dynamics, La Jolla, California, Mar 2006*, arXiv:nucl-th/0606022.
[23] A. M. Poskanzer and S. A. Voloshin, Phys. Rev. C **58**, 1671 (1998).
[24] P. Sorensen [STAR Collaboration], *19th International Conference on Ultra-Relativistic Nucleus-Nucleus Collisions: Quark Matter 2006 (QM2006), Shanghai, China, 14-20 Nov 2006*; arXiv:nucl-ex/0612021.
[25] P. F. Kolb, J. Sollfrank and U. W. Heinz, Phys. Rev. C **62**, 054909 (2000).
[26] E. Beebe, J. Alessi, A. Kponou, A. Pikin, K. Prelec, G. Kuznetsov and M. Tiunov, AIP Conf. Proc. **572** (2000) 43; J. G. Alessi *et al.*, *Proceedings of 2005 Particle Accelerator Conference, Knoxville, Tennessee, USA, May 16-20, 2005*, p. 363-365.